# Supplementary Appendix

This appendix has been provided by the authors to give readers additional information about their work.

Supplement to: Bar KJ, Sneller MC, Harrison LJ, et al. Effect of HIV antibody VRC01 on viral rebound after treatment interruption. N Engl J Med 2016;375:2037-50. DOI: 10.1056/NEJMoa1608243

**SUPPLEMENTARY APPENDIX**

# Effect of HIV antibody VRC01 on viral rebound after treatment interruption

Katharine J. Bar, Michael C. Sneller, Linda J. Harrison, J. Shawn Justement, Edgar T. Overton, Mary E. Petrone, D. Brenda Salantes, Catherine A. Seamon, Benjamin Scheinfeld, Richard W. Kwan, Gerald H. Learn, Michael A. Proschan, Edward F. Kreider, Jana Blazkova, Mark Bardsley, Eric W. Refsland, Michael Messer, Katherine E. Clarridge, Nancy Tustin, Patrick J. Madden, KaSaundra Oden, Sijy J. O'Dell, Bernadette Jarocki, Andrea R. Shiakolas, Randall L. Tressler, Nicole A. Doria-Rose, Robert T. Bailer, Julie E. Ledgerwood, Edmund Capparelli, Rebecca M. Lynch, Barney S. Graham, Susan Moir, Richard A. Koup, John R. Mascola, James A. Hoxie, Anthony S. Fauci, Pablo Tebas, and Tae-Wook Chun.

**TABLE OF CONTENTS**

## Supplementary Methods

### Study inclusion criteria

A5340: A5340 enrolled HIV-1 infected individuals, ages ≥18 years, with a $CD4^+$ T-cell count of ≥450 cells/$mm^3$, an undetectable plasma viral load (<50 copies/mL) for at least 24 weeks, $CD4^+$ T-cell nadir >200 cells/$mm^3$, and no known treatment with ART during acute or early infection. In addition to HIV-specific criteria, exclusion criteria included known treatment during acute infection, previous receipt of a humanized or human monoclonal antibody (mAb), treatment with systematic glucocorticoids or other immunomodulators, active hepatitis B or C virus infection, ongoing opportunistic infection(s), history of an AIDS-defining illness, history of severe allergic reactions, abnormal laboratory values, inadequate venous access, and weight >115 or <53 kg. A plasma or serum specimen before the initiation of antiretroviral therapy (ART) was required for at least 8 participants. A5340 excluded participants receiving non-nucleoside reverse transcriptase inhibitor (NNRTI) based ART due to the prolonged half-life of those drugs and the potential risk for development of resistance[25,26] upon discontinuation of the drug by requiring a stable protease inhibitor (PI)- or integrase inhibitor (INSTI)- based regimen for 24 weeks

NIH trial: The NIH trial enrolled HIV-1 infected individuals, ages ≥18 years, with a $CD4^+$ T-cell count of ≥450 cells/$mm^3$ and an undetectable plasma viral load (<50 copies/mL) for at least or 3 years. HIV-infected individuals enrolled in the study had been receiving continuous ART resulting in suppression of plasma viremia below the limit of assay detection for a minimum of 3 years and maintenance of a $CD4^+$ T-cell count greater than 450 cells/$mm^3$. Study subjects receiving non-nucleoside reverse transcriptase inhibitors (NNRTIs) were switched to an integrase inhibitor-based regimen 2 weeks prior to the first infusion of VRC01 to prevent

development of NNRTI-resistance. The NIH study participants receiving NNRTIs were switched to an INSTI-based regimen 2 weeks prior to ATI.

**Study drug**

VRC01 was isolated from B cells of a chronically HIV-infected individual who maintained low levels of plasma viremia without receiving ART. VRC01 used in both trials was produced under the current good manufacturing practice (cGMP) by Leidos Biomedical Research, Inc., Frederick, Maryland, under contract to the Vaccine Research Center at the National Institute of Allergy and Infectious Diseases. The 40 mg/kg dosing strategy was chosen based on the observed 14 day half-life in aviremic HIV-infected individuals in prior trials[1,2].

**Adverse Events Monitoring**

A5340: Diagnosis, signs and symptoms, and laboratory results were graded using version 2.0 of the Division of AIDS (DAIDS) adverse events (AEs) grading table, and assessed for relationship to VRC01 by the core study team. Post-entry, sites were required to report all signs and symptoms of grade 2 of higher, as well as all solicited signs and symptoms that were grade <2 from an infusion report card asking participants about injection site pain, redness, swelling and induration, as well as systematic AEs like feeling unwell, muscle aches, headache and chills during the 7 days after receipt of the antibody. All diagnoses identified by the ACTG criteria for clinical events and other diseases were additionally required to be reported. DAIDS AEs grading table described at: http://rsc.tech-res.com/safetyandpharmacovigilance/gradingtables.aspx. ACTG criteria described at http://reprievetrial.org/wp-content/uploads/2014/11/Appendix100.pdf.

NIH trial: Diagnosis, signs and symptoms, and laboratory results were graded using version 2.0 of the DAIDS adverse events (AEs) grading table, and assessed for relationship to VRC01 by the Principal Investigator. All AE were recorded in a computerized database using the definitions for AE, SAE, and Unanticipated Problems given in the NIH HRPP Standard Operating Procedure number 16 (available at http://ohsr.od.nih.gov/OHSR/pnppublic.php).

**Historical ACTG data on control analytical treatment interruption group**

There have been six previous ACTG clinical trials that have utilized analytical treatment interruptions (ATI). A total of 61 participants were on suppressive non-NNRTI ART started during chronic infection and received no immunologic interventions. At week 4 of the ATI the proportion of participants with virologic suppression <200 copies/mL was 13% (8/61), and at week 8 it was 3% (2/61)[3]. For the comparison with historical controls we used participants in ACTG trials that were receiving non-NNRTI-based regimens because of the prolonged half-life of NNRTIs artificially delayed the return of viremia.

**Power calculations**

A5340: We planned to enroll 15 participants; all receiving VRC01. We assumed a 15% loss to follow-up or non-protocol required study treatment discontinuation, to have a total of 13 evaluable participants for planned per-protocol analysis, using the binomial distribution and the conservative assumption that in the absence of an intervention 90% will have a return of viremia within 8 weeks of treatment interruption, we had 95% power to detect a difference of 40% (i.e., return of viremia by 8 weeks in 50%) using a two-sided test with a significance level of 0.10. Regarding the assessment of safety, the sample size of 15 VRC01-treated participants would

provide a 90% probability of observing a VRC01-related AE that would occur in 14% or more of treated participants. After enrollment of 13 evaluable participants for the primary efficacy analysis, recruitment was stopped with a total of 14 participants receiving VRC01.

NIH trial: The sample size of our study was 30. The sample size was selected based on the primary endpoint of the study (safety). A sample size of 30 patients provided a 95.8% chance of observing an adverse event with a 10% probability or greater. The study also included futility criteria for plasma viral rebound following discontinuation of ART. Futility guidelines were based on the number of patients who would meet criteria to restart ART following treatment interruption. We used Bayesian methodology whereby we calculated that if 10 of the first 10 subjects experienced plasma viral rebound while receiving VRC01, there was a >70% chance that the true rebound rate was >90%, at which point futility would be declared and study enrollment would be stopped.

**Trial outcome analysis**

Both trials: for analysis of time to first confirmed HIV-1 RNA ≥200 copies/mL during the ATI, HIV-1 RNA measurements were binned at the nearest scheduled week. The cumulative probability of remaining virologically suppressed (i.e. no confirmed HIV-1 RNA ≥200 copies/mL) was calculated by Kaplan-Meier methods. The A5340 analysis was designed to exclude the historical control probability of 90% from the exact 90% CI of the proportion of participants with return of viremia within 8 weeks of the ATI. At the time of design, the historical control was based on 6 prior ACTG treatment interruption trials, as well as the SMART study. When Jonathan Li and colleagues published a formal pooled analysis of these 6 prior ACTG trials in January 2016[3], the SAP was amended to include a formal comparison to the

non-NNRTI control group. Comparison to historical ACTG data was by the two-sided Fisher's exact test.

A5340: Spearman's rank correlations coefficients were calculated to assess the relationship between pre-ART and study entry variables with time to first confirmed HIV-1 RNA ≥200 copies/mL. One participant was excluded from viral rebound evaluation, as he discontinued ART prematurely and had plasma viremia of 50,600 copies/mL at the time of VRC01 infusion. Per protocol, his ART was restarted one week later upon confirmation of viremia. Notably, his plasma viral load decreased ~100-fold to 520 copies/ml in the 7 days post-infusion before restarting ART (Participant A11, Fig S3), supporting the previously reported antiviral effect of VRC01 in viremic individuals[2].

NIH trial: Study participants received infusions of VRC01 (40mg/kg) intravenously 3 days prior to and 14 and 28 days following cessation of ART, and monthly thereafter. Plasma viremia and $CD4^+$ T-cell counts were measured at baseline (Day -3) and subsequently as shown in Fig. 1. Study subjects who met any of the following criteria discontinued VRC01 infusions and resumed ART: 1) a greater than 30% decline in baseline CD4 T-cell count or an absolute $CD4^+$ T-cell count below 350 cells/$mm^3$; 2) a sustained (≥4 weeks) HIV plasma viremia greater than 1,000 copies/mL: 3) any HIV-related symptoms; or 4) pregnancy. Study subjects were not pre-screened for sensitivity or resistance of their virus to neutralization by VRC01. The primary end point of the study was safety, as defined by the rate of occurrence of grade 3 or higher adverse events (AE), including serious AE (SAE), that were possibly related to infusion of VRC01. The secondary end point was virologic efficacy, as defined by the number of study subjects who experienced plasma viral rebound or who met the immunologic or clinical criteria to discontinue VRC01 infusions and restart ART.

**VRC01 plasma concentration measurements and modeling**

Quantification of VRC01 concentrations in participant plasma and individual participant noncompartmental PK analysis were performed as previously described[2]. Briefly, VRC01 serum concentration quantification was performed in 96-well plates on a Beckman Biomek–based automation platform using the anti-idiotype mAb 5C9. Pharmacokinetic data were fit to a two-compartment population model using the computer program NONMEM (Ver 7.2).

**Anti-drug antibody assay**

Antidrug antibody analysis was performed as previously described[1]. Briefly, a Meso Scale Discovery (MSD) electrochemiluminescence (ECL) bridging assay was used to screen for the presence of VRC01 anti-idiotypic antibodies in serum from baseline and at week 8 of the ATI in A5340. Detection of anti-drug antibodies was achieved by a homgeneous solution phase overnight incubation of diluted serum sample along with biotinylated and SULFO-TAG labeled drug and formed a complex. Biotin-labeled VRC01 served as a capture molecule on a streptavidin pre-coated MSD plate and the SUFO-TAG labeled VRC01 was the reported used for detection.

**<u>A5340</u> Analyses Methods:**

**Viral RNA extraction, cDNA synthesis, single genome sequencing (SGS)**

SGS enables proportional representation of the complex HIV-1 virus quasispecies with linkage across the sequenced region with minimal *in vitro* errors[4]. Viral RNA extraction, cDNA synthesis, and SGS were performed to amplify gp41 or gp160 *env* as previously described[4,5].

Amplicons were directly sequenced and chromatograms were inspected for evidence of priming from multiple templates or introduction of PCR error in early cycles.

**Phylogenetic analyses**

Sequences from each participant were aligned using ClustalW[6] and alignments were adjusted as necessary by visual inspection. Regions in within-participant alignments that could not be unambiguously aligned were removed from subsequent phylogenetic analyses. Maximum-likelihood phylograms for each participant were inferred using PhyML Version 3[7], which jointly estimates the tree and the parameters of the evolutionary model. Evolutionary model classes for within-participant data sets were selected using jModelTest version 2.1.4[7,8] using the AICc criterion[9]. Within-participant alignments were aligned sequentially using ClustalW. Hypervariable regions as defined in Los Alamos National Laboratory HIV Sequence Database Variable Region Characteristics webtool (http://www.hiv.lanl.gov/content/sequence/VAR_REG_CHAR/) and other regions that could not be unambiguously aligned were removed from the alignment used for the phylogenetic analysis encompassing all of the sequences (Fig. S7). Pairwise diversity estimates were performed by DIVEIN[10]. Assessment for phylogenetic clustering within individual participant's sequences was performed by Slatkin-Maddison and Hudson's nearest neighbor tests[11-13]. To determine the clonality of rebound viremia, sequences were analyzed by a previously described model of neutral virus evolution[4,14], which assumes virus undergoes rapid expansion without selection. Under this model, low-diversity sequence lineages display a star-like phylogeny and a Poisson distribution of mutations, coalesce to an unambiguous founder sequence enabling estimates of time from a most recent common ancestor (MRCA)[4,14 15]. Pairwise nucleotide Hamming

distances were calculated using code from the Los Alamos National Laboratory HIV database Poisson Fitter version 2 tool. In calculating Hamming distances, gaps were excluded. For rebound virus populations that met these criteria ($p>0.05$ in goodness-of-fit to Poisson distribution), recent clonal expansion from a single virus was interpreted to indicate a single virus rebounded from latency to found systemic virus replication during rebound. If rebound sequences violated the conditions of this model, it was interpreted that more than one virus rebounded from latency to found rebound viremia (Fig. S9). All sequences were deposited in GenBank (accession numbers: KX587007-KX587459 for A5340 and KX517915-KX518294 for NIH trial).

**VRC01 antibody footprint sequence analysis**

Modified longitudinal logo plots were generated with the Longitudinal Antigenic Sequences and Sites from Intra-host Evolution (LASSIE) tool[16]. All sequences were compared to the rebound consensus sequence, whether rebound was monoclonal or polyclonal. The consensus was generated as a majority-rule consensus using sequences from the earliest time point post-rebound and treating gaps as characters (ambiguous sites were denoted with an "X"). Intact N-linked glycosylation sequons (NXS/T, where X is any amino acid other than proline) were designated as "O"s (OXS/T). Env residues in Loop D, CD4 binding loop, β20/β21 regions, and the base of V5 that are known VRC01 contact residues[17] were included. Residues were colored as follows: acidic residues (ED) in red, basic residues (HKR) in dark blue, asparagines within N-linked glycosylation sequons (O) in cyan, and all other amino acids in black. To emphasize differences between pre-ATI viruses and rebound viruses and highlight that little or no sequence

evolution in the VRC01 footprint was observed post-rebound, residues that match the rebound consensus/master were replaced with white space.

**Env gene cloning and pseudovirus production**

Select *env* sequences from throughout the pre-ART phylogeny and those representing the consensus sequence of low-diversity rebound lineages were molecularly cloned for the production of pseudovirus and phenotypic analyses as described previously[4,5]. Briefly, to reduce the probability of generating molecular *env* clones with *Taq* polymerase errors, we reamplified from the first-round PCR product under the same nested PCR conditions but used only 25 cycles. Correctly sized amplicons identified by gel electrophoresis were gel-purified by using the QIAquick gel purification kit according to the recommendations of the manufacturer (Qiagen), ligated into the pcDNA3.1 Directional Topo vector (Life Technologies) and transformed into competent TOP10 *E. coli* bacteria. Bacteria were plated on LB agar plates supplemented with 100 μg/ml ampicillin and cultured at 25°C for 3 days. Single colonies were selected and grown overnight in liquid LB broth at 30°C with 225 rpm shaking followed by plasmid isolation. Finally, each molecular clone was sequence-confirmed to be identical to the previously determined *env* sequence of the plasma *env* amplicon.

Pseudovirus was prepared by transfecting overnight cultured $3x10^6$ 293T cells in $10cm^2$ tissue culture dishes with 4 μg of *rev/env* expression plasmid and 4 μg of HIV-1 backbone: using Fugene 6 (Roche Applied Science, Indianapolis, IN). Pseudovirus containing culture supernatants were harvested 2 days after transfection, cleared of cellular debris by low-speed centrifugation and stored in aliquots at -80°C. Viruses were titrated on TZM-bl reporter cells (8129; NIH AIDS Research and Reference Reagent Program), which contain a Tat-inducible

luciferase and a β-galactosidase gene expression cassette. Infectious titers were measured on 24-well plates based on β-galactosidase production, representing the number of infection events per μL of virus stock (IU/μL) as described previously[18].

**Neutralization assays**

Virus neutralization by VRC01 was assessed on TZM-bl cells as described previously[18]. TZM-bl cells were seeded at $1x10^4$ per well and cultured in 96-well plates overnight. Virus stocks dilutions were made to final concentrations of DMEM containing 6% FBS and 40 μg/mL DEAE-dextran (Sigma-Aldrich, St. Louis, MO) to achieve 2000 IU/well. Equal volume virus dilutions and two to five-fold serially diluted mAbs were mixed and incubated at 37°C for 1 h. Supernatants were then removed and 80 μL of these mixtures were added. Media-only and virus-only control wells were included as background and 100% infectivity, respectively. Luciferase activity was measured after 48 h incubation in 37°C using Bright-Glo per the manufacturer's instructions (Promega). All assays were done in triplicate in each of at least two independent experiments. To calculate the concentration of antibody that neutralized 50% ($IC_{50}$), and 80% ($IC_{80}$), of virus infection the antibody dose-response curves were fit with a four-parameter logistic regression equation using Prism 5.0 (GraphPad Software Inc. San Diego, CA). When 50% or 80% neutralization was not achieved at the 50 μg/mL concentration of VRC01, the $IC_{50}$ or $IC_{80}$ was recorded as 50 μg/mL.

**VRC01 neutralization resistance analysis**

For comparison of pre-ART and rebound VRC01 resistance by cloned Envs, multilevel random-effects models (random intercept and slope) were fitted to account for multiple clones

per participant at each time-point, and a two-sided p-value for the estimated difference in pre-ART and rebound resistance was calculated. Analysis was performed on the log10 scale. For analysis, $IC_{50}$ values were truncated at 25 μg/mL and $IC_{80}$ values were truncated at 50 μg/mL. For comparison of pre-ART $IC_{50}$ in A5340 to an historical subtype B panel, a random-effects model (random intercepts) was fitted to account for multiple clones per participant in A5340, and a two-sided p-value for the estimated difference was calculated. Analyses were performed in SAS version 9.4.

**NIH Trial Analyses Methods:**

**Measurements of HIV reservoirs**

In order to determine the frequency of cells carrying HIV DNA at baseline, genomic DNA was isolated from highly enriched $CD4^+$ T-cells and subjected to droplet digital PCR (Bio-Rad Laboratories) according to the manufacturer's specifications. The amplification reaction was carried out using HIV-specific and RPP30 (housekeeping gene)-specific primers and probes. The following primers were used for amplification of HIV LTR: 5'- GRAACCCACTGCTTAAGC CTCAA -3' (5' primer) and 5'- TGTTCGGGCGCCACTGCTAGAGA -3' (3' primer) along with the fluorescent probe 5'-6FAM-AGTAGTGTGTGCCCGTCTGTT-IABkFQ-3'. The following primers were used for amplification of RPP30: 5'-GATTTGGACCTGCGAGCG-3' (5' primer) and 5'-GCGGCTGTCTCCACAAGT-3' (3' primer) along with the fluorescent probe 5'-HEX-TTCTGACCTGAAGGCTCTGCGC-IABkFQ-3'.

**Neutralization assays for replication-competent HIV isolates prior to and following infusions of VRC01 and discontinuation of ART**

In order to determine the capacity of VRC01 to neutralize autologous, infectious virus, we generated multiple replication-competent HIV isolates from study subjects at two time-points: prior to the first infusion of VRC01 and at the time of viral rebound. Replicate wells containing low input numbers of CD8-depleted peripheral blood mononuclear cells (PBMCs) isolated from study subjects were stimulated with anti-CD3 antibody in IL-2 containing media for 2-3 days, followed by co-culture with CD8-depleted $CD4^+$ T cell blasts generated from HIV-seronegative healthy donors. Following a culture period of up to 10 days, cell-free supernatants were harvested and the concentration of the virus was determined by HIV p24 ELISA (Perkin Elmer). Infectious HIV (0.1- 0.2ng of HIV p24) was incubated with 10μg/ml of VRC01 or other bNAbs (3BNC-117, 10-1074, and PGT121, all obtained from NIH AIDS Reagent Program), or an anti-CD4 antibody that binds to a region near the CDR-2 region of domain 1 of CD4 receptor (UB-421, United BioPharma, Taiwan)[19], or human IgG (negative control) in duplicate for 90 minutes. The antibody-HIV complex was then added to TZM-bl cells in each well of 96-well flat bottom plates. Following a 2-day incubation period, cells were lysed and viral infectivity was quantitated by measuring luciferase activity (Promega) in a luminometer (Tecan). For each viral isolate, the suppression by test antibody was calculated as % luciferase activity over control antibody (human IgG).

**Determination of $IC_{80}$ of bNAbs VRC01, 3BNC117, 10-1074, and PGT121 against autologous, infectious HIV isolates**

Neutralization of autologous, infectious isolates by VRC01, 3BNC117, 10-1074, and PGT121 was assessed as previously described[2]. Briefly, each infectious HIV isolate was titrated by serial dilutions and infection of TZM-bl cells. The viral isolates and monoclonal antibodies

were then incubated in a 96-well plate at 37°C for 30 min before addition of TZM-bl cells. After 2 days of incubation, cells were lysed and the viral infectivity was quantified by measuring luciferase activity using a luminometer. Neutralization curves were fit by nonlinear regression using a 5-parameter hill slope equation. The $IC_{80}$ values were reported as the antibody concentrations required to suppress infection by 80%.

**Single genome amplification (SGA) and cloning of HIV gp160 *env* genes**

Virion-associated viral RNA in plasma was subjected to amplification and cloning of HIV *env* genes as previously described with the following modifications[4,20]. Viral RNA was extracted using the QIAmp viral RNA mini kit (Qiagen) according to the manufacturer's instructions. For samples with plasma viremia <1,500 copies/ml, virions were concentrated from 1-2 mLs of plasma by centrifugation. cDNA was generated by incubating 30 μl template RNA with 3 μl 10mM dNTPs and 0.75 μl of 20 μM antisense primer 3'envBout (TTGCTACTTGTGATTGCTCCATG) for 5 min at 65°C to denature the RNA followed by reverse transcription using SuperScript III reverse transcriptase (Life Technologies) according to the manufacturer's instructions in a 60 μL total reaction volume. Amplification of HIV *env* genes was performed by nested PCR using the Platinum Taq High Fidelity polymerase (Life Technologies) as previously described[2]. In order to ensure a majority of sequences would be generated from a single template, cDNA was diluted so that PCR positive wells were < 30% of the total products. Single cDNA templates were amplified in a 35-cycle first round PCR with forward and reverse primers envB5out (TAGAGCCCTGGAAGCATCCAGGAAG) and envB3out (TTGCTACTTGTGATTGCTCCATG) followed by a 45-cycle second round PCR containing 1 μl of first round product and forward and reverse primers envB5in

(CACCTTAGGCATCTCCTATGGCAGGAAGAAG) and envB3in (GTCTCGAGATACTGCTCCCACCC). Amplicons were run on precast 1% agarose gels (Embi Tec) and sequenced. Sequences that contained stop codons, large deletions, or mixed bases were removed from further analysis. Sequences were codon aligned using MUSCLE in the Geneious suite (version 8.1.7), manually refined and gap-stripped. Phylogenetic trees were inferred using maximum likelihood/rapid bootstrapping in RAxML version 8 run on the Cyberinfrastructure for Phylogenetic Research (CIPRES) Science Gateway. Trees were visualized mid-point rooted using MEGA version 6[21] and bootstraps greater than 70 are shown. Sequence changes between time points were quantified by uploading protein alignments to the neutralization-based epitope prediction algorithm (https://exon.niaid.nih.gov/nep/). Pre-ART sequences were assigned a value of "0" and post-infusion sequences were assigned a value of "50" and potency threshold was set to 25. The result was a rank order of positions using normalized mutual information to calculate sites of variation[22,23]. All sequences were deposited in GenBank (accession numbers: KX587007-KX587459 for A5340 and KX517915-KX518294 for NIH trial).

**Statistical Methods**

For each study subject, the mean percent suppression of pre-infusion viral isolates by VRC01 was computed and a weighted average was determined using the number of observations per study subject as weights. The same approach was used for 3BNC117, 10-1074, PGT121, and UB-421 and the difference between the weighted averages for the percent suppression by VRC01 and the above antibodies were computed. A paired permutation test was applied to obtain a p-value for the difference in percent suppression by VRC01 versus each other bNAb. The test involved randomly reversing or not reversing the per-subject averages of viral

suppression by VRC01 versus another bNAb to obtain a reference distribution. A similar permutation approach was conducted for the level of suppression of pre- versus post-infusion viral isolates by VRC01 except that the switching involved pre- versus post-infusion suppression percentages for a given patient. The weight assigned to a study subject was proportional to 1/m+1/n, where m and n were the numbers of pre- and post-infusion measurements, respectively. Additionally, an individual responder analysis was conducted using the Wilcoxon/Mann-Whitney test to determine whether a given study subject had a statistically significant change from pre- to post-infusion.

**Details of Adverse Events**

A5340: No grade 3 or higher AEs were reported. No grade 2 VRC01-related AEs were reported. Two grade 1 VRC01-related AEs were reported in 2 participants; an IV site induration and itchiness of the left antecubital fossa. Five post-entry grade 2 non-VRC01-related AEs were reported in 4 participants. A detailed list of adverse events in the ACTG A5340 trial is shown in Table 1.

**Table 1: Adverse events in ACTG A5340 trial**

| Study Participant | MedDRA Term | Grade | Relationship* |
|---|---|---|---|
| A01 | Infusion site induration | 1 | Treatment Related Event |
| A04 | Cough | 1 | Non-Treatment Related Event |
| | Nasal congestion | 1 | Non-Treatment Related Event |
| | Postnasal drip | 1 | Non-Treatment Related Event |
| | Sinus congestion | 1 | Non-Treatment Related Event |
| | Sore throat | 1 | Non-Treatment Related Event |
| | Wheezing | 1 | Non-Treatment Related Event |
| | Viral upper respiratory tract infection | 2 | Non-Treatment Related Event |
| A07 | Glucose high | 1 | Non-Treatment Related Event |
| | Glucose high | 2 | Non-Treatment Related Event |
| | Phosphate abnormal NOS | 1 | Non-Treatment Related Event |
| | Glucose high | 2 | Ongoing Non-Treatment Related Event |
| A08 | Extremities itchy sensation of | 1 | Treatment Related Event |
| A09 | Headache | 2 | Non-Treatment Related Event |
| A13 | Cervical radiculopathy | 2 | Baseline |
| | Numbness localized | 2 | Baseline |
| A14 | Onychomycosis | 2 | Non-Treatment Related Event |

*investigators' assessment, treatment=VRC01

NIH trial: No serious adverse events related to VRC01 were reported. One serious adverse event occurred during the protocol. Nausea and vomiting occurred following alcohol consumption in one study subject (N03) 21 days after VRC01 infusion and precipitated an overnight hospital admission for observation. One episode of Grade 3 neutropenia occurred in

this same study subject four months after last dose of VRC01. This subject had documented intermittent grade 2/3 benign neutropenia prior to study enrollment. A detailed list of adverse events in the NIH trial is shown in Table 2.

**Table 2: Adverse events in NIH trial**

| Study Participant | MedDRA Term | Grade | Relationship* |
|---|---|---|---|
| N01 | Chest pain | 1 | Unrelated to VRC01 |
| | Localized edema | 1 | Unlikely related to VRC01 |
| | Rash | 1 | Unlikely related to VRC01 |
| | Difficulty sleeping | 1 | Unrelated to VRC01 |
| | Calcium low | 1 | Unlikely related to VRC01 |
| | Sodium decreased | 1 | Unrelated to VRC01 |
| N02 | Tinea versicolor | 1 | Unlikely related to VRC01 |
| N03 | Nausea | 2 | Unlikely related to VRC01 |
| | Vomiting | 1 | Unlikely related to VRC01 |
| | Neutrophil count decreased | 3 | Unlikely related to VRC01 |
| | Blood phosphate decreased | 2 | Unlikely related to VRC01 |
| N04 | Calcium low | 2 | Unlikely related to VRC01 |
| N05 | ALT increased | 1 | Unlikely related to VRC01 |
| | ALT increased | 1 | Unlikely related to VRC01 |
| | AST increased | 1 | Unlikely related to VRC01 |
| | Traveller's diarrhea | 2 | Unrelated to VRC01 |
| N06 | Blood glucose increased | 2 | Unlikely related to VRC01 |
| | Hyperglycemia | 1 | Unrelated to VRC01 |
| N07 | Acute nasopharyngitis (common cold) | 1 | Unlikely related to VRC01 |
| | Blood bicarbonate low | 1 | Unrelated to VRC01 |
| N08 | Blood glucose increased | 1 | Unlikely related to VRC01 |
| | Blood phosphate decreased | 1 | Unlikely related to VRC01 |
| N09 | Dry cough | 1 | Unlikely related to VRC01 |
| | Rhinorrhea | 1 | Unlikely related to VRC01 |
| | Herpes simplex | 1 | Unlikely related to VRC01 |
| | Sinus congestion | 1 | Unrelated to VRC01 |
| | Sore throat | 1 | Unrelated to VRC01 |
| N10 | Flu-like symptoms | 2 | Unlikely related to VRC01 |

*investigators' assessment

## Supplementary Figures

### Figure S1. $CD4^+$ and $CD8^+$ T-cell counts of study participants (NIH trial)

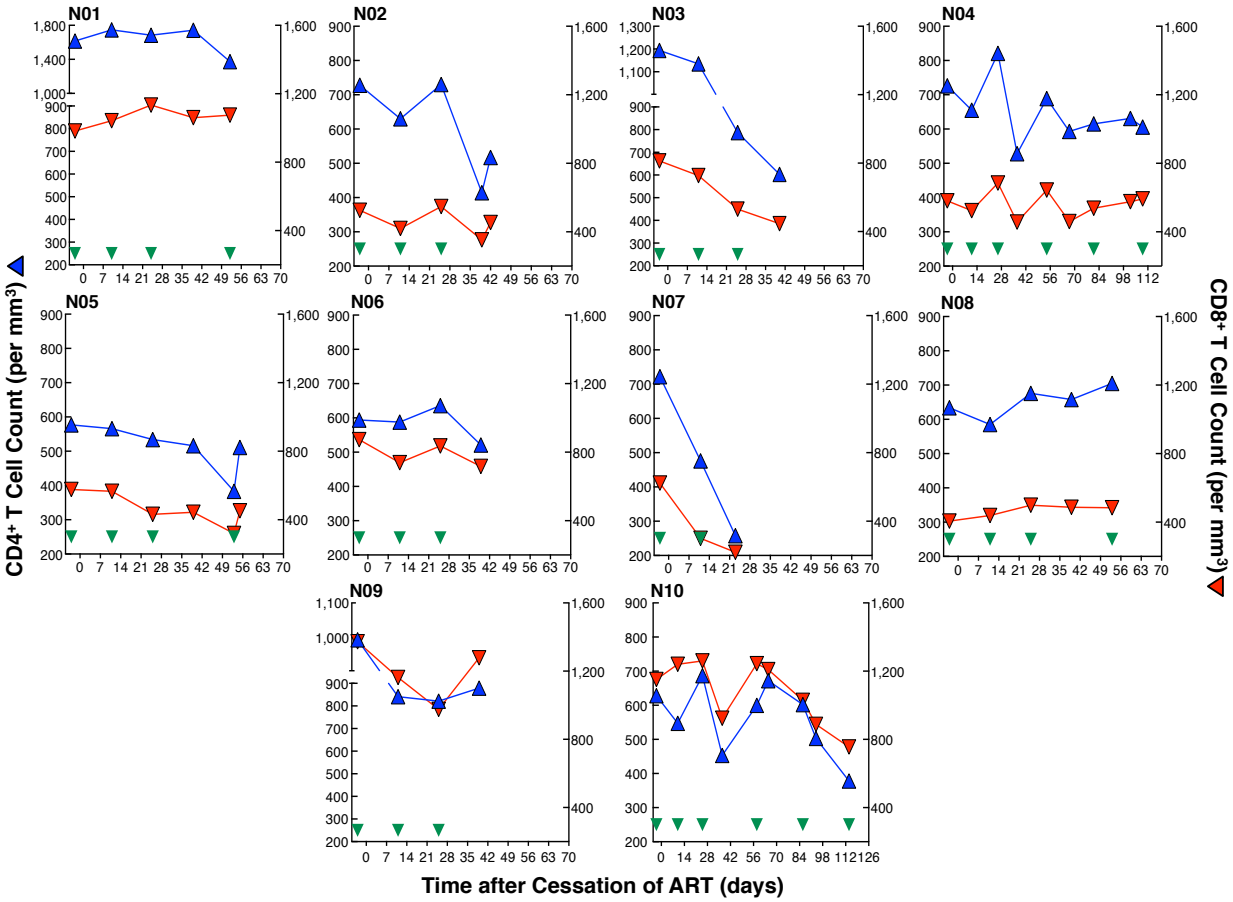


$CD4^+$ (blue triangles) and $CD8^+$ (red triangles) T-cell counts are shown for each study subject at baseline and following infusions of VRC01 and discontinuation of ART. Green triangles indicate day of VRC01 infusion.

**Figure S2. Frequencies of HIV proviral DNA in $CD4^+$ T-cells of study participants at baseline (NIH trial)**

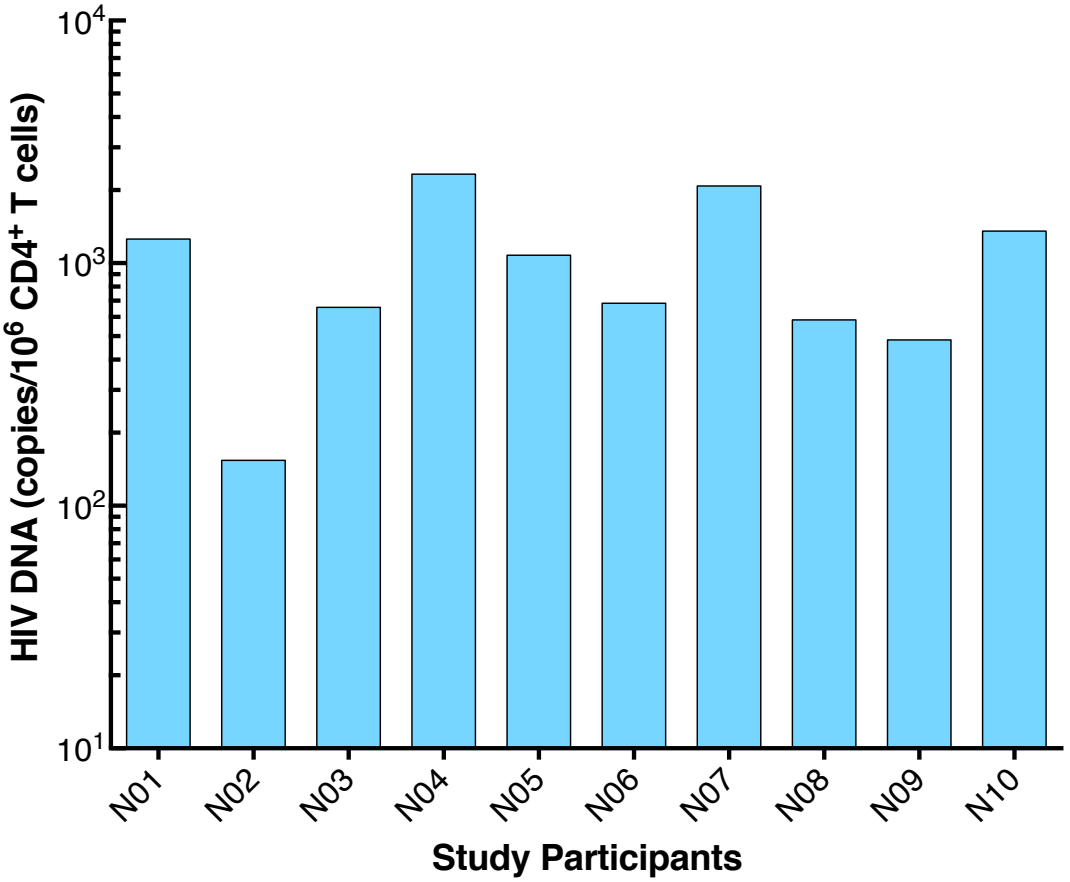


Levels of HIV proviral DNA in the $CD4^+$ T-cells, determined by droplet digital PCR, are shown for each study participant at baseline.

**Figure S3. Plasma viral loads and VRC01 concentration for the 14 study participants (A5340)**

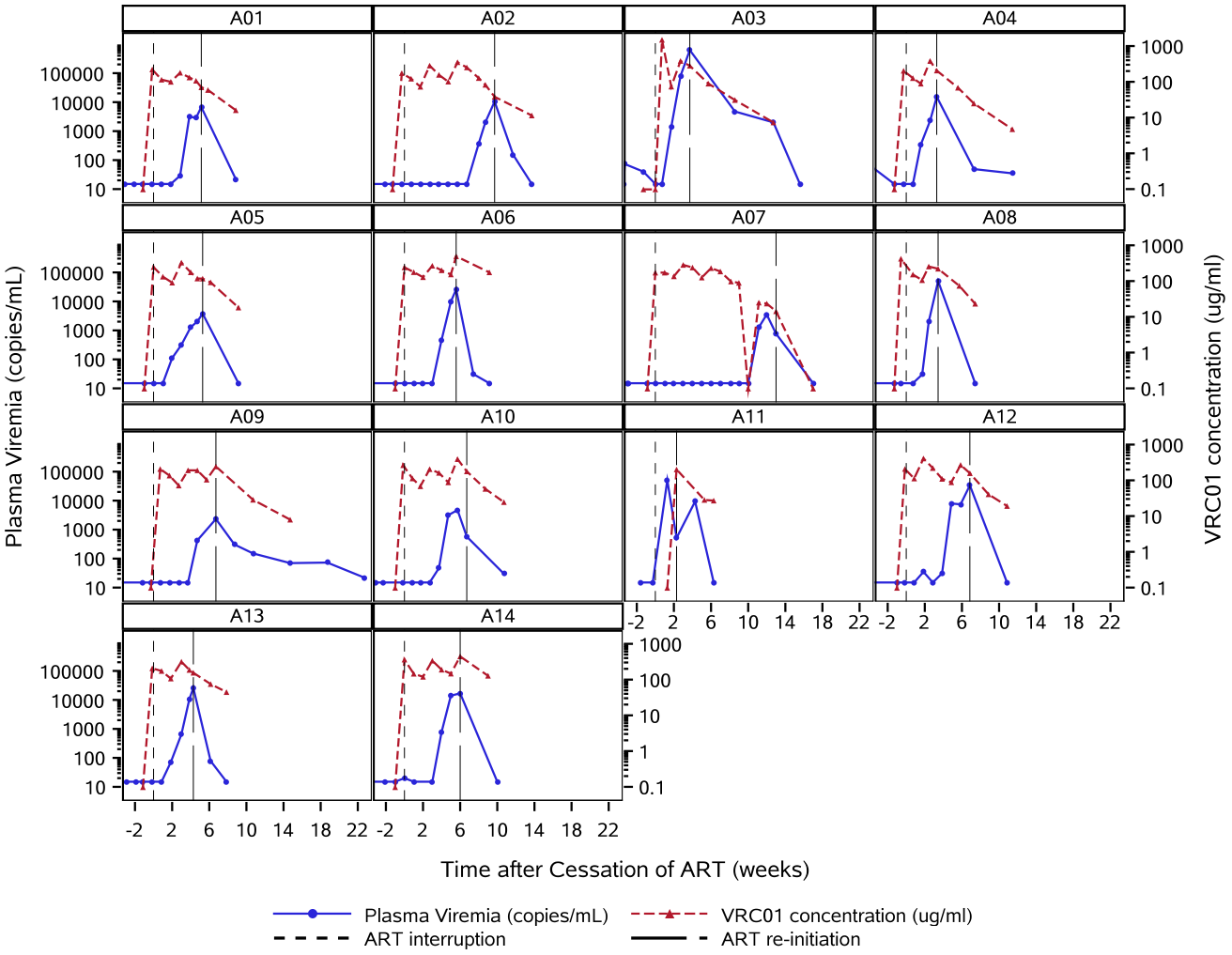


Weekly HIV-1 RNA levels for each of the 14 enrolled participants are shown in blue ($log_{10}$ scale shown on left) and measured plasma VRC01 concentrations are shown in red ($log_{10}$ scale on right) over time after ATI. ART interruption is shown by shorter dashed line and ART reinitiation is shown by longer dashed lines. Note that participant A11's study time frame is shifted to match his actual date of ATI. He reported discontinuing his ART 1 week prior to his first VRC01 infusion and had undetectable plasma HIV-1 RNA at -2 and 0 weeks before this date and measured HIV-1 RNA of 50,600 copies/mL one week after his ART interruption on the

date of his first VRC01 infusion. Following VRC01 administration, his plasma HIV-1 RNA dropped to 520 copies/mL within 1 week, at which point he was restarted on ART per protocol.

**Figure S4. Correlations between baseline characteristics and time to viral rebound (A5340)**

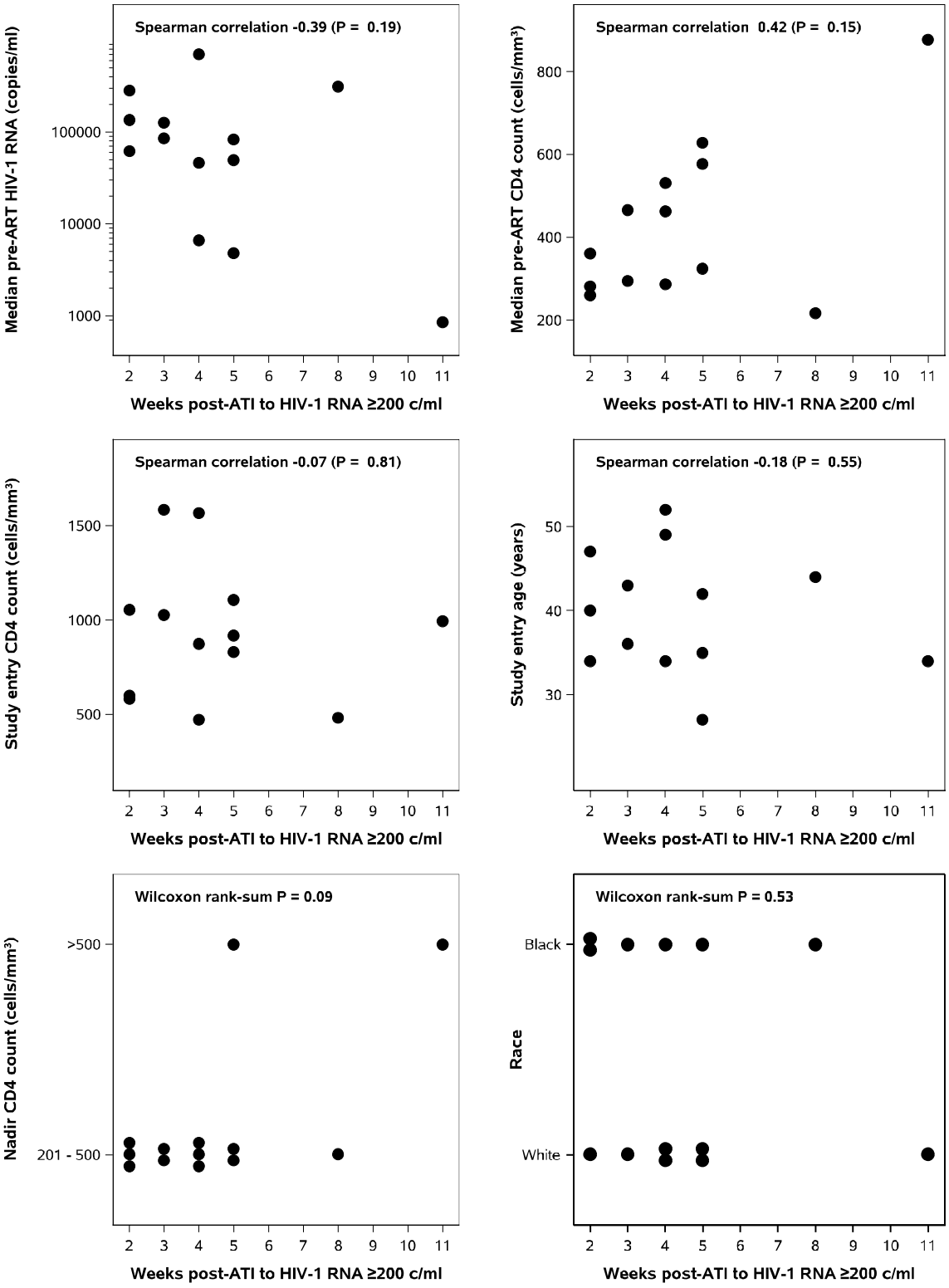

As exploratory analyses, the relationship between baseline characteristics and time to rebound was assessed. Median pre-ART HIV-1 plasma RNA level and median pre-ART CD4 T-cell count were weakly correlated with time to rebound (Spearman correlations of -0.39 (P=0.19) and 0.42 (P=0.15), respectively), while entry CD4 and age were not correlated. There was a trend (two-sided exact Wilcoxon rank-sum P=0.09) to longer time to rebound for participants with higher nadir CD4 (>500 cells/$mm^3$), but no difference was seen for race.

**Figure S5. Pharmacokinetics of VRC01 and plasma viremia of study participants (NIH trial)**

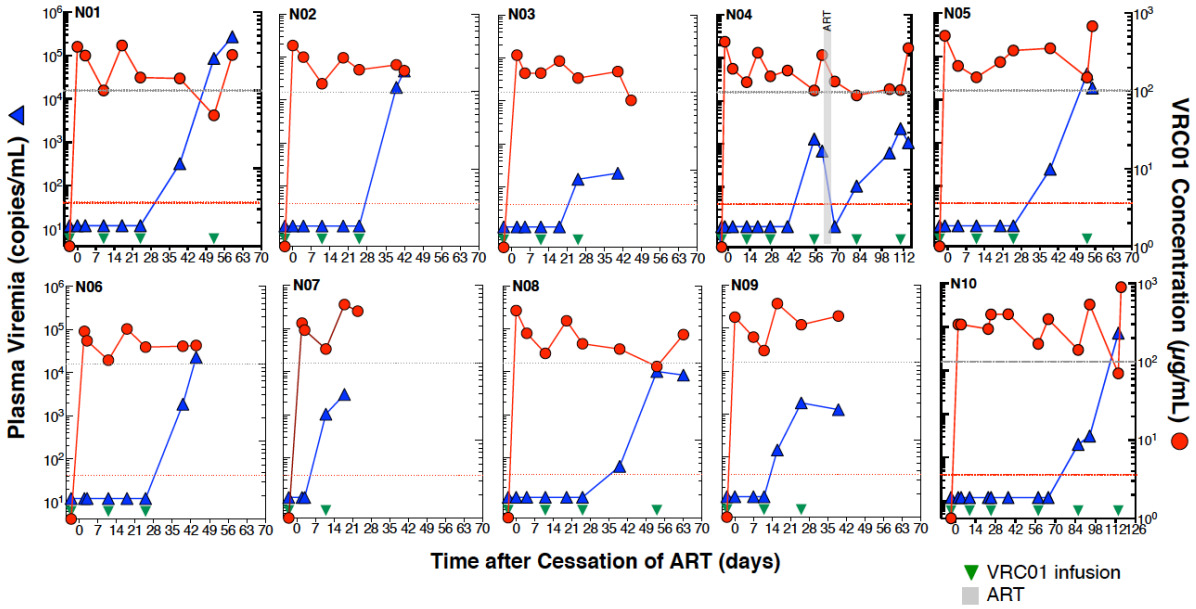


*In vivo* plasma levels of VRC01 and HIV are shown for each study participant. The green triangles indicate infusion time points of VRC01. Grey dotted lines are shown at 100μg/mL of VRC01. The limit of detection of VRC01 was <0.98μg/mL. Red dotted lines indicate the detection limit of HIV plasma viremia (40 copies/mL).

**Figure S6. VRC01 levels and pharmacokinetic modeling (A5340)**

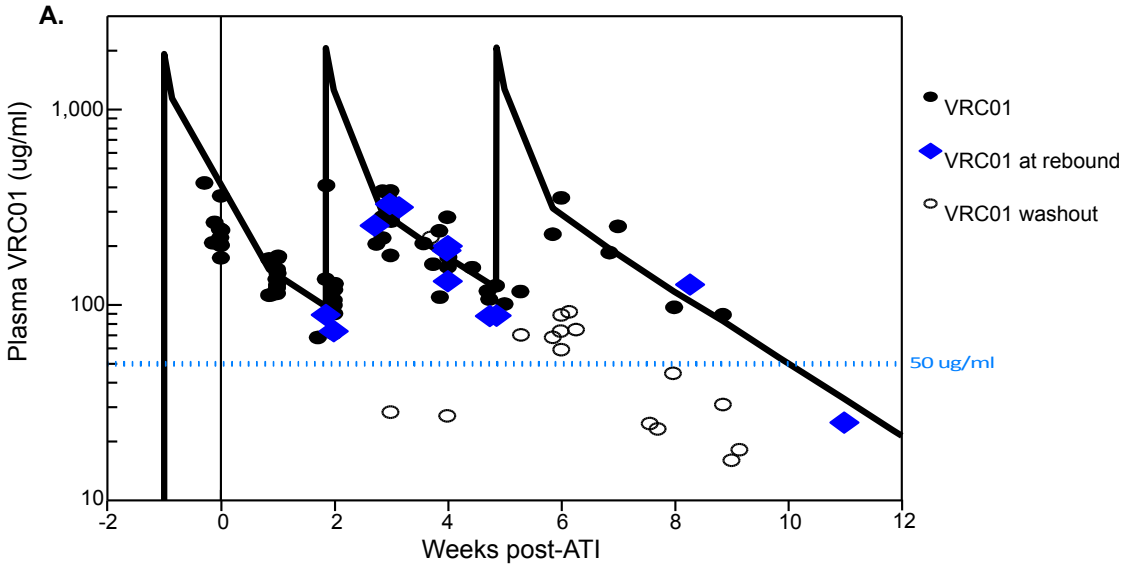


Plasma concentrations of VRC01 for all participants are plotted against time of ATI. All participants maintained plasma levels of VRC01 greater than 50 μg/mL for more than 8 weeks and 12/13 participants experienced viral rebound with these levels. Solid black squares indicate measured levels before viral rebound; open squares were obtained after viral rebound. The blue squares indicate levels of VRC01 at the time point of first detectable viremia. Modeling of VRC01 pharmacokinetics shown by black line.

**Figure S7. Maximum likelihood phylogenetic tree of participants' pre-ART and rebound *env* sequences (A5340)**

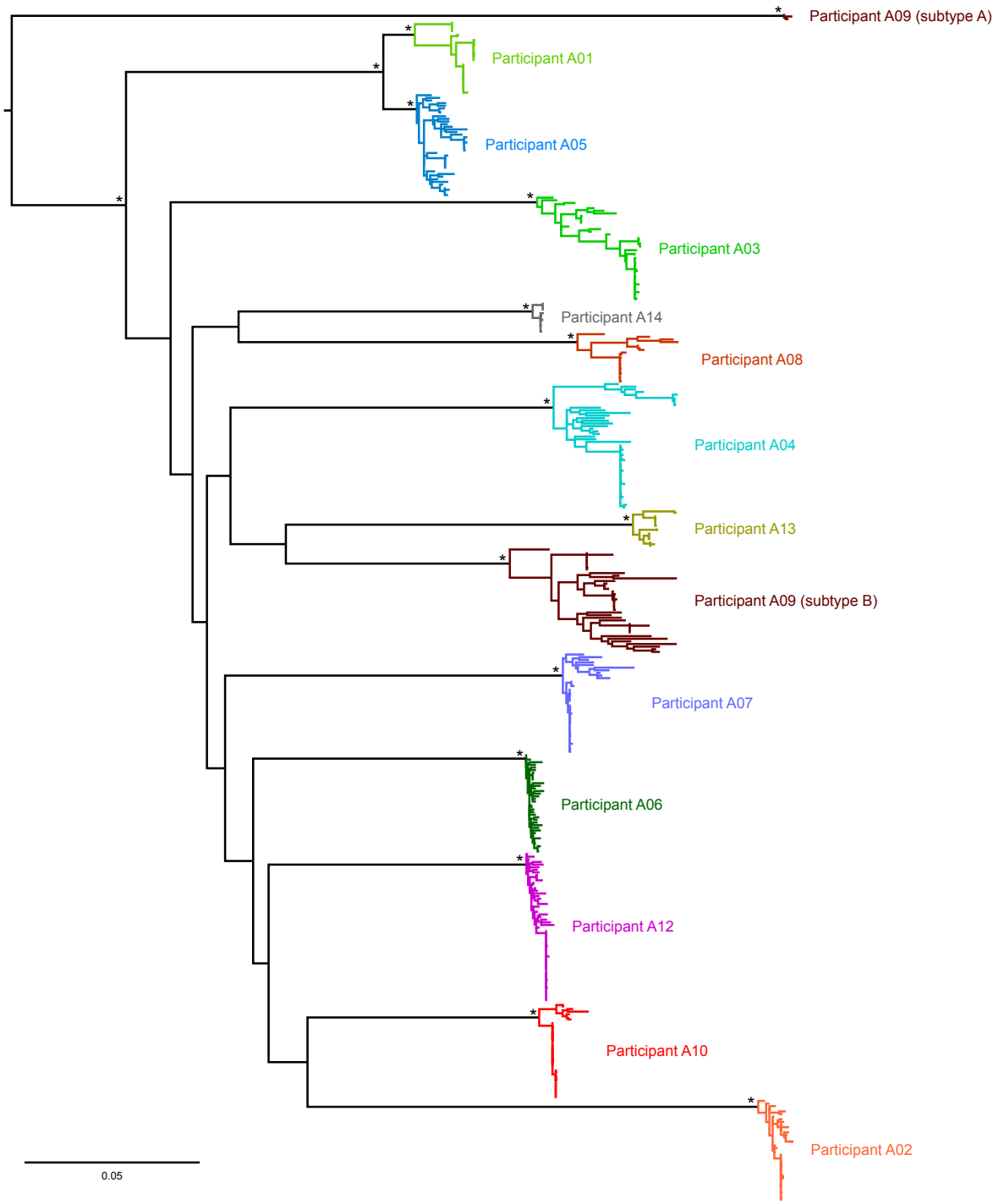

All pre-ART and rebound gp160 *env* sequences from the 13 A5340 participants evaluated for viral rebound were analyzed in a maximum likelihood phylogenetic tree. Each participant's sequences cluster independently in monophyletic lineages, with one exception. Participant A09 has pre-ART virus quasispecies is comprised of both Subtype A and Subtype B viruses, as well as a single sequence that appears to be a recombinant (by Highlighter plot and Recco analyses[24]). Participant A09's rebound sequences are all Subtype B and cluster with his Subtype B pre-ART viruses. Participants 1 and 5 are relatively closely related with consensus sequences differing by approximately 3%, but their lineages cluster independently with bootstrap support of 64%. Bootstrap support values of 100% are shown using asterisks. For the sake of clarity, bootstrap values within participants' clades are not shown, except for Participant 9 who was infected with two Subtypes. The independence of each participant's lineage demonstrates the lack of laboratory cross-contamination and the genetic relatedness of pre-ART plasma and rebound sequences. The scale bar represents 0.05 substitutions/site.

**Figure S8. Maximum Likelihood phylogenetic trees of individual participants (A5340)**

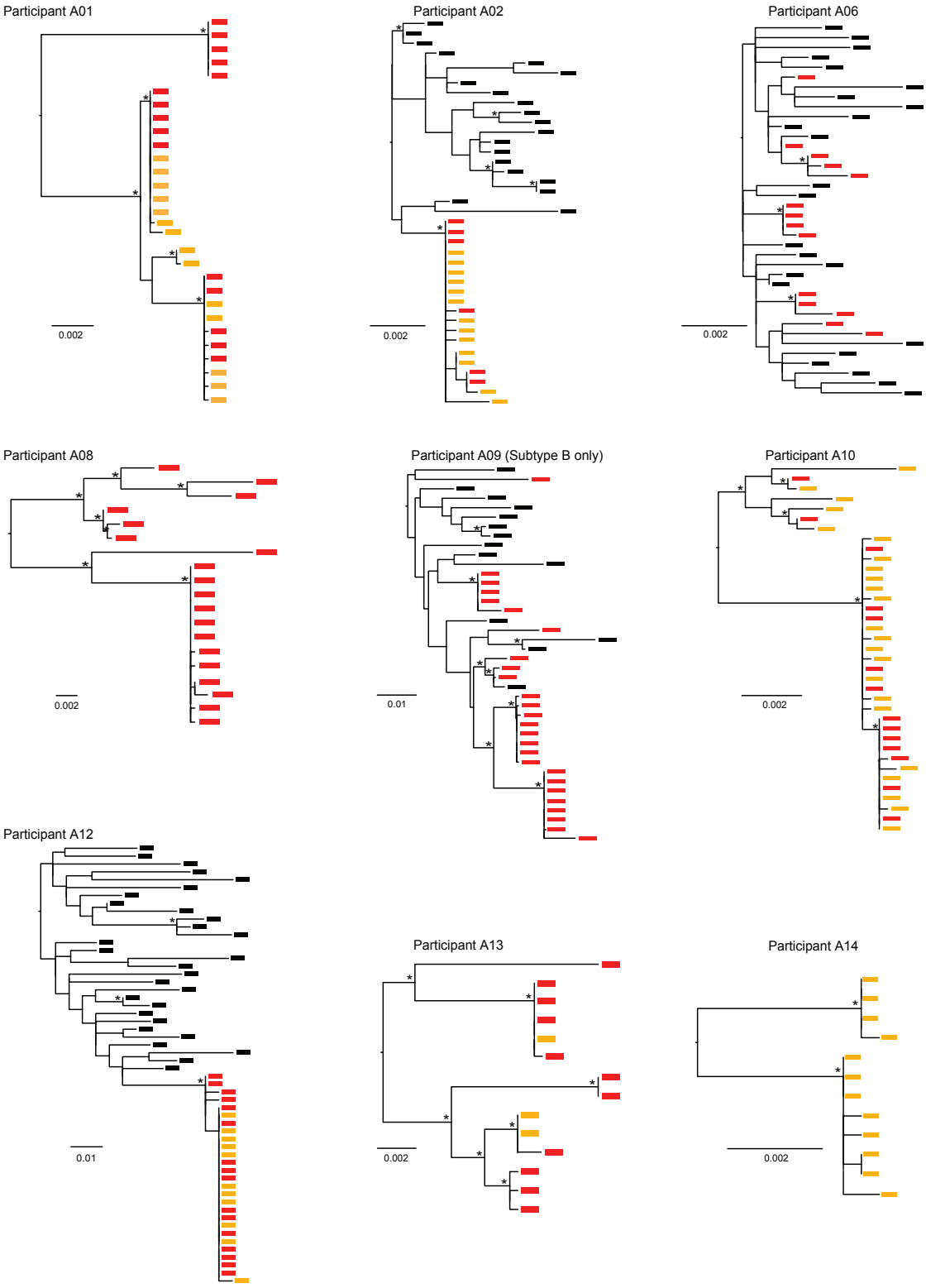

Maximum likelihood phylogenetic trees of gp160 *env* sequences from participants not displayed in Figure 3 are shown, except Participant 11, whose sequences were not evaluated due to early discontinuation of ART. Pre-ART sequences are shown in black, rebound sequences from weeks 1 and 2 of detectable viremia are shown in red and orange, respectively. Genetic distance scale bars are shown for each tree and bootstrap support >70% is shown with asterisks. Pre-ART plasma was not available in participants A01, A08, A10, A13, A14. For participant A09, only the Subtype B sequences are displayed here to allow for assessment of the relatively smaller genetic distances between the pre-ART and rebound subtype B sequences. Monoclonal rebound lineages are seen in participants A02 and A12. Polyclonal lineages are seen in participants A01, A06, A08, A09, A10, A13, and A14.

**Figure S9. Poisson Fitter analyses for participants with pre-ART and rebound samples (A5340)**

| | | First time point plasma SGS | | | | | |
|---|---|---|---|---|---|---|---|
| Participant | Single rebound? | # SGS | Min HD | Mean HD | Max HD | p | p (no APOBEC) |
| A01 | no | 29 | 0 | 34.210 | 64 | N/A | N/A |
| A02 | yes | 19 | 0 | 1.637 | 7 | 0.7082 | 0.5125 |
| A03 | no | 27 | 0 | 30.321 | 52 | N/A | N/A |
| A04 | yes | 26 | 0 | 2.380 | 8 | 0.6405 | 0.5389 |
| A05 | no | 15 | 0 | 18.756 | 39 | N/A | N/A |
| A06 | no | 14 | 0 | 8.110 | 15 | N/A | N/A |
| A07 | no | 28 | 0 | 4.154 | 10 | 2.06E-07 | 0.0144 |
| A08 | no | 19 | 0 | 33.789 | 84 | N/A | N/A |
| A09 | no | 26 | 0 | 46.563 | 98 | N/A | N/A |
| A10 | no | 37 | 0 | 7.648 | 29 | N/A | N/A |
| A12 | yes | 27 | 0 | 0.853 | 4 | 0.4617 | 0.834 |
| A13 | no | 14 | 0 | 24.182 | 40 | N/A | N/A |
| A14 | no | 12 | 0 | 9.667 | 17 | N/A | N/A |

To determine the clonality of rebound viremia, sequences were analyzed by a previously described model of neutral virus evolution[4,14], which assumes virus undergoes exponential expansion without selection. Under this model, low-diversity sequence lineages display a star-like phylogeny and a Poisson distribution of mutations and coalesce to an unambiguous founder sequence enabling estimates of time from a most recent common ancestor (MRCA)[4,14]. Pairwise nucleotide Hamming distances were calculated using code from the Los Alamos National Laboratory HIV database Poisson Fitter tool version 2. The rebound virus populations from participant A02, A04, and A12 met these criteria ($p>0.05$ in goodness-of-fit to Poisson distribution), indicating recent clonal expansion from a single virus. These low-diversity lineages that fit model criteria indicate that a single virus rebounded from latency to found systemic virus replication during rebound. Participant A07 demonstrated 2 closely related

rebound virus populations, but modeling suggests that the genetic diversity present at the first week of rebound could not have arisen from a single virus. The low p value (0.05) indicates multiple viruses were required to lead to the genetic diversity present at this time, supporting polyclonal rebound in this participant. "# SGS" indicates the number of single genome sequencing-derived gp160 env sequences used in the analysis, "HD" is Hamming Distance, "p" indicates p value for goodness-of-fit to Poisson distribution, "p (no APOBEC)" indicates analysis with sequence positions with APOBEC-hypermutation sites removed.

**Figure S10. VRC01 antibody footprint sequence changes from pre-ART to rebound (A5340)**

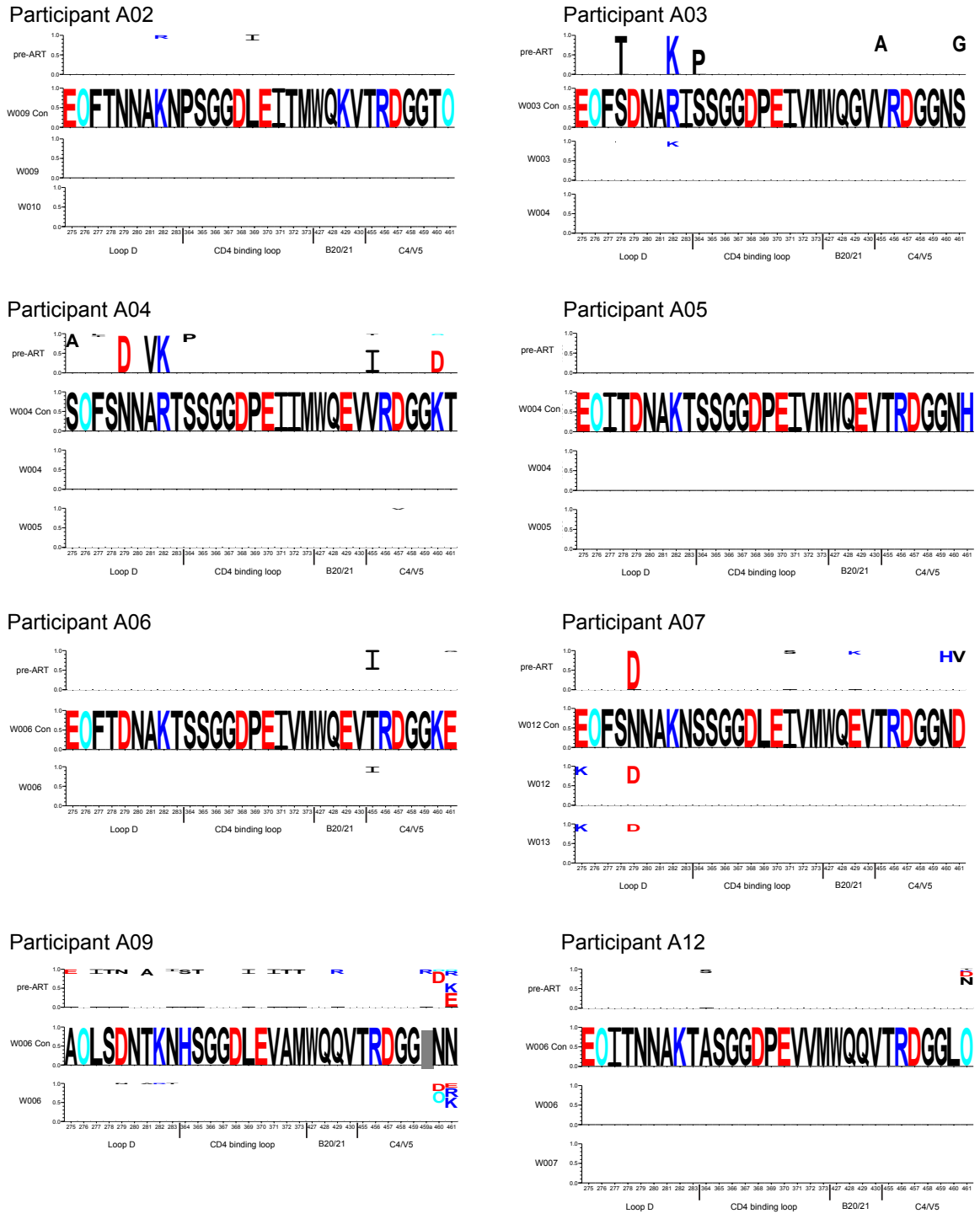

To analyze changes in the predicted VRC01 antibody binding regions between pre-ART and rebound virus populations, modified longitudinal logo plots were generated with the Longitudinal Antigenic Sequences and Sites from Intra-host Evolution (LASSIE) tool[16]. The VRC01 binding footprint was represented by Env residues in Loop D, CD4 binding loop, β20/β21 regions, and the base of V5 that are known VRC01 contact residues[17]. All sequences were compared to the consensus of the rebound viruses, which is displayed as color-coded, bold letters in the second line. The top line shows amino acid differences in the pre-ART sequences from the rebound consensus. The consensus was generated as a majority-rule consensus using sequences from the earliest time point post-rebound. Residues were colored as follows: acidic residues (ED) in red, basic residues (HKR) in dark blue, asparagines within N-linked glycosylation sequons (NXS/T, depicted as an "O") in cyan, and all other amino acids in black. Gaps are treated as characters. Several participants, including participants A03 and A04, show substantial changes in the binding footprint between the pre-ART and rebound sequences, suggesting selection for a minor variant to arise in rebound. Other participants show minimal changes in the binding footprint. Between week 1 and 2 of rebound, minimal changes are seen within the VRC01 binding footprint.

**Figure S11. Sequence analysis of pre-ART and post-VRC01 infusion HIV *env* in plasma (NIH)**

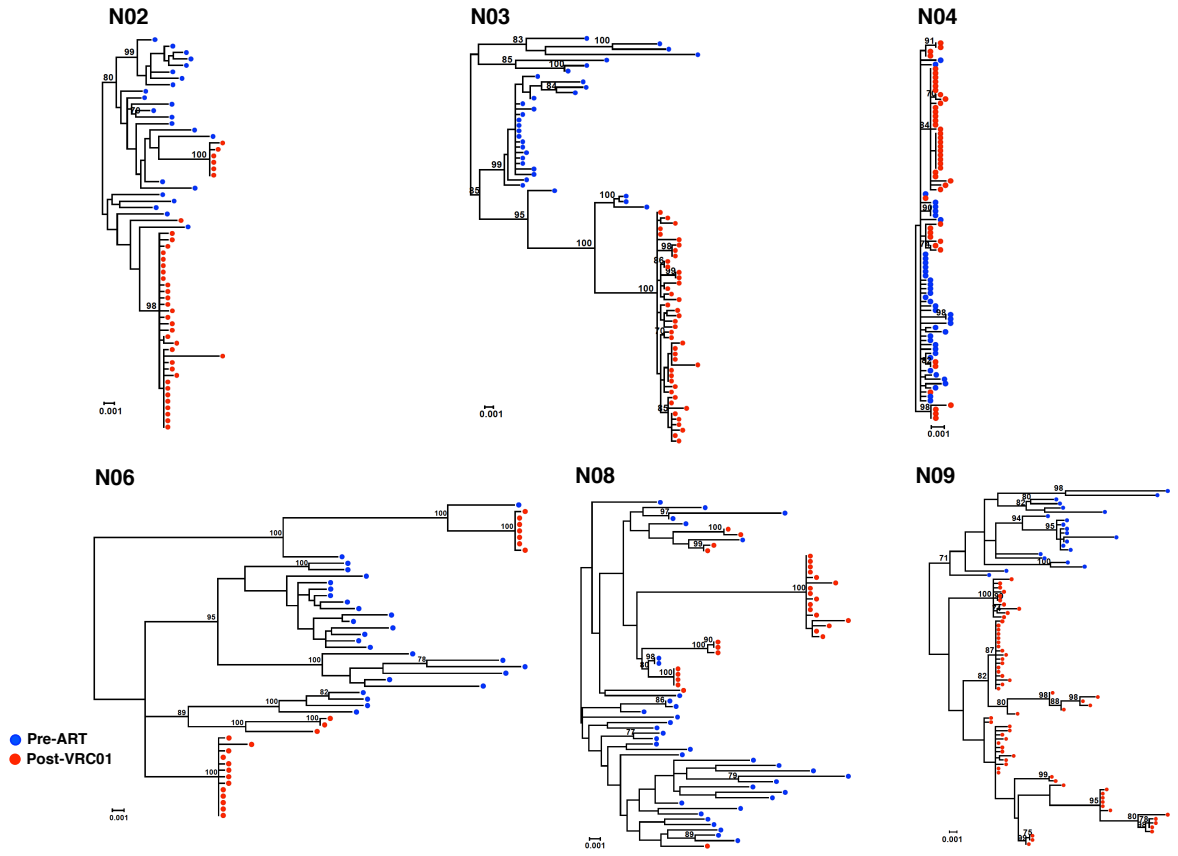


Viral RNA from pre-ART (blue circles) and post-VRC01 infusion (red circles) plasma was used to generate maximum likelihood phylogenetic trees from single genome amplification of HIV *env*. The phylogenetic trees were midpoint rooted for visualization and each colored symbol indicates a single amplicon. Bootstrap values >70 are shown with scale indicating genetic distance.

**Figure S12. Sequence analysis of pre-ART and post-VRC01 infusion HIV *env* in plasma**

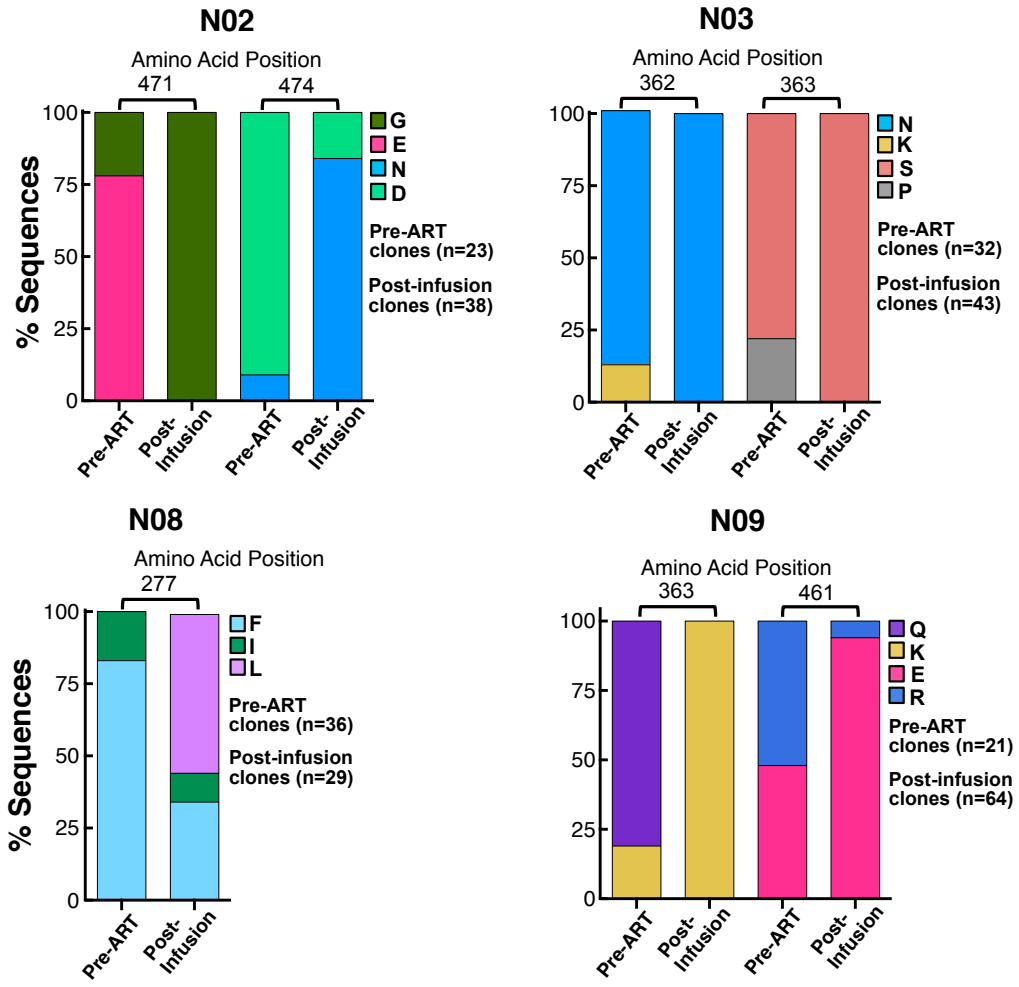


HIV *env* protein sequences were aligned and analyzed using a neutralization-based epitope prediction (NEP) algorithm (exon.niaid.nih.gov) to calculate a rank order of positions that were significantly different between time points. Changes in amino acid residues that occurred within or next to the VRC01 epitope are shown by bar graphs for subjects V02, V03, V08 and V09 and indicate the percent of sequences that contain the specified amino acid. Amino acid residue numbers are based on HIV HXB2 numbering and the total number of pre-ART or post-infusion sequences is indicated.

**Figure S13. VRC01-resistance of pre-ART and rebound viruses**

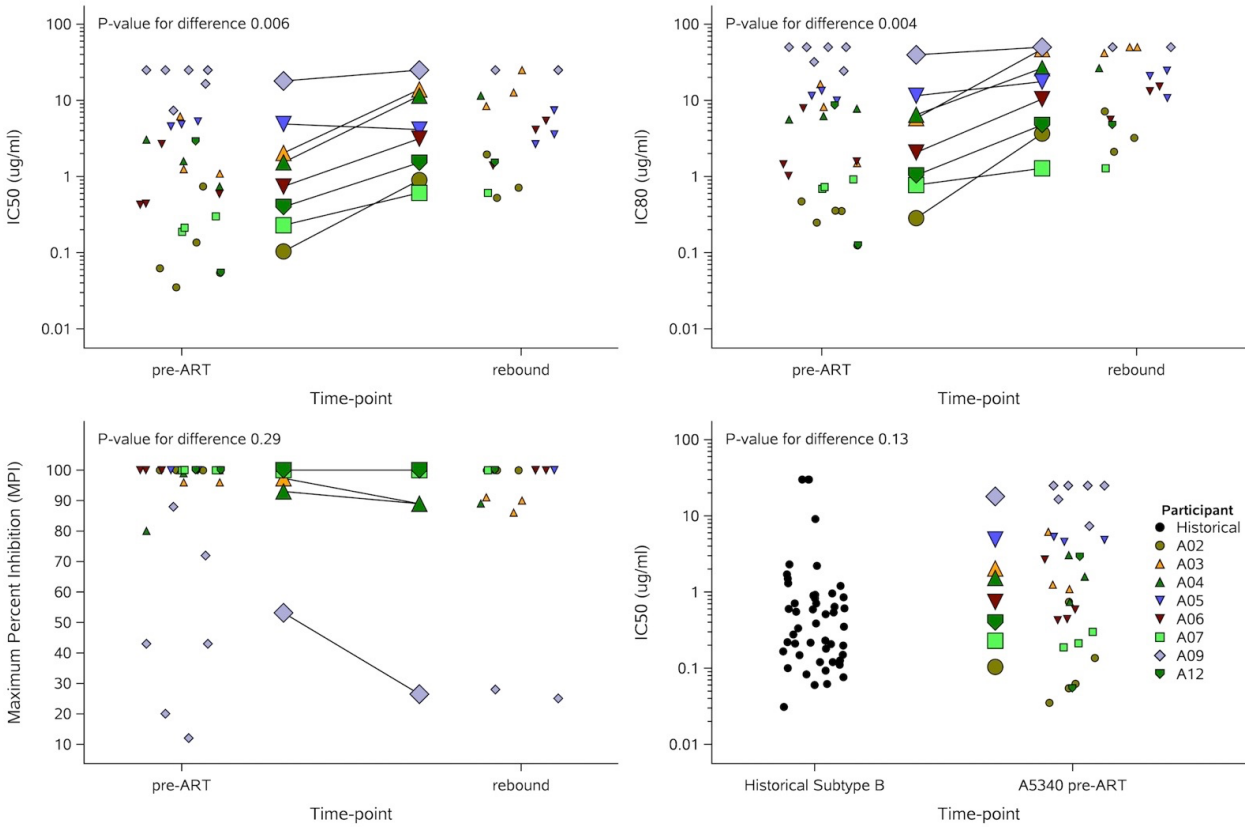


Pre-ART and rebound Envs from the eight participants with available samples were compared for changes in neutralization sensitivity by $IC_{50}$ (truncated at 25 µg/mL), $IC_{80}$ (truncated at 50 µg/mL) and MPI. Individual Env titers were plotted laterally, while the mean titers per participant were compared between time points centrally. A. By $IC_{50}$, there was a 3.44 fold increase (two-sided random-effects model p value=0.006). B. By $IC_{80}$, there was a 3.79 fold increase (two-sided random-effects model p value of 0.004). C. No change seen in MPI. D. There was a statistically non-significant trend towards increased resistance comparing the Pre-ART IC50 titers for the eight A5340 participants (represented as mean of each participant's individual Envs) to the 49 subtype B Envs reported in the 2010 report initially characterizing VRC01[25], two-sided random-effects model p=0.13.

**Figure S14. Neutralization sensitivity of autologous, infectious HIV isolates prior to and following infusions of VRC01 and discontinuation of ART**

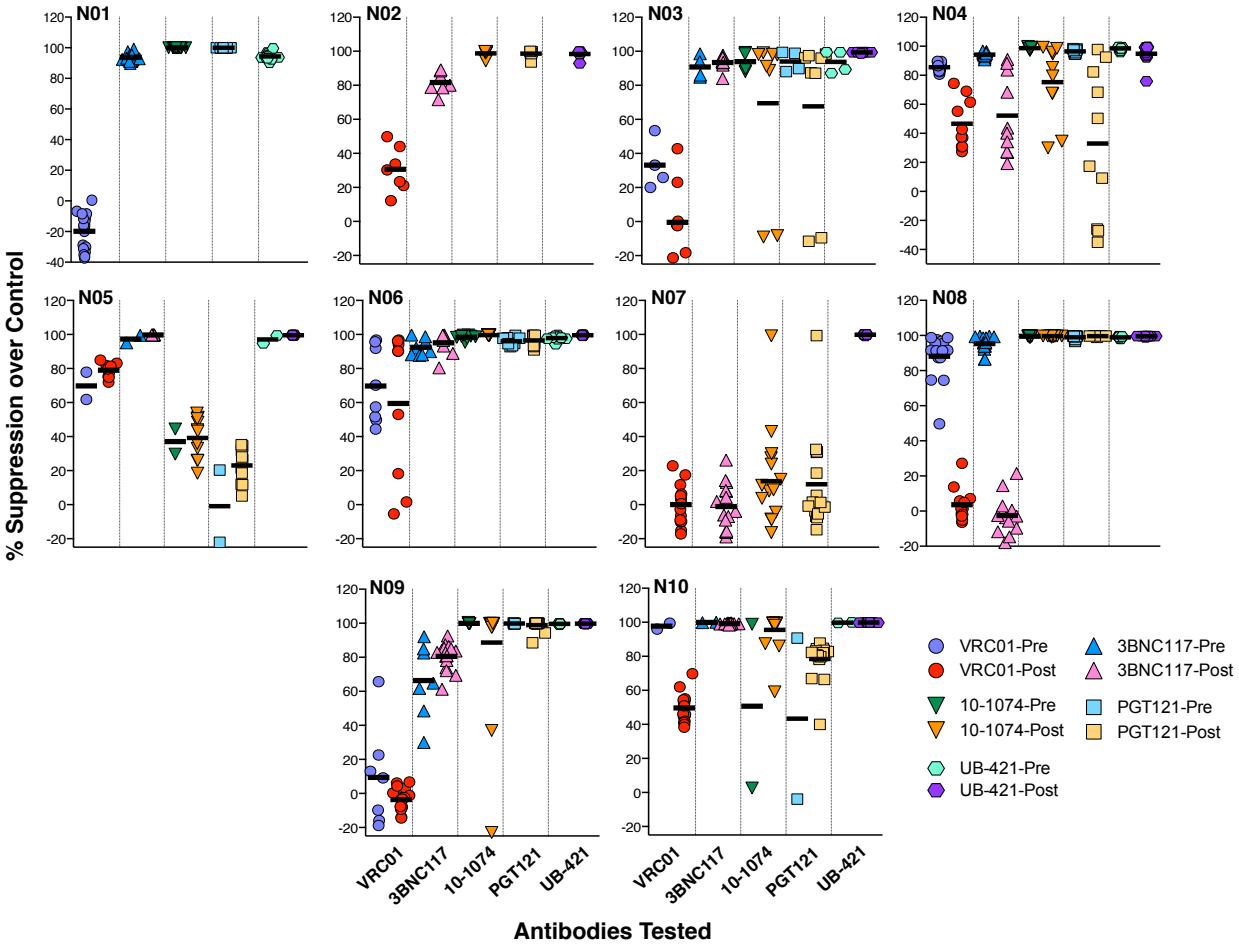


Neutralization of pre- and post-infusion infectious viral isolates by VRC01, other bNAbs (3BNC117, 10-1074, and PGT121), and UB-421 is shown for each study participant. Black horizontal bars depict mean values.

## Figure S15. Neutralization of pre- and post-infusion viral isolates by bNAbs

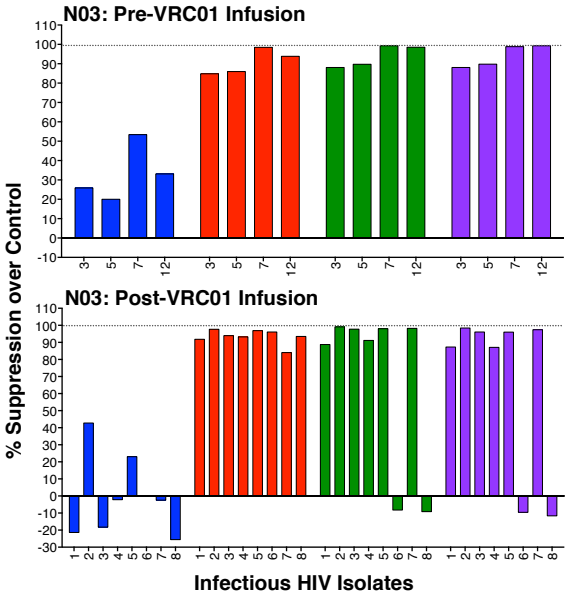


**N03 $IC_{80}$ (μg/mL)**

| Time Point | Infectious HIV Isolates | VRC01 | 3BNC117 | 10-1074 | PGT121 |
|---|---|---|---|---|---|
| Pre-VRC01 Infusion | 7 | 30.1 | 3.69 | 2.04 | 1.39 |
| | 12 | >40 | 7.71 | 4.19 | 1.85 |
| Post-VRC01 Infusion | 1 | >40 | 6.72 | 3.41 | 2.27 |
| | 3 | >40 | 5.76 | 2.66 | 1.62 |
| | 5 | >40 | 5.85 | 3.84 | 2.27 |
| | 8 | >40 | 6.9 | >40 | >40 |

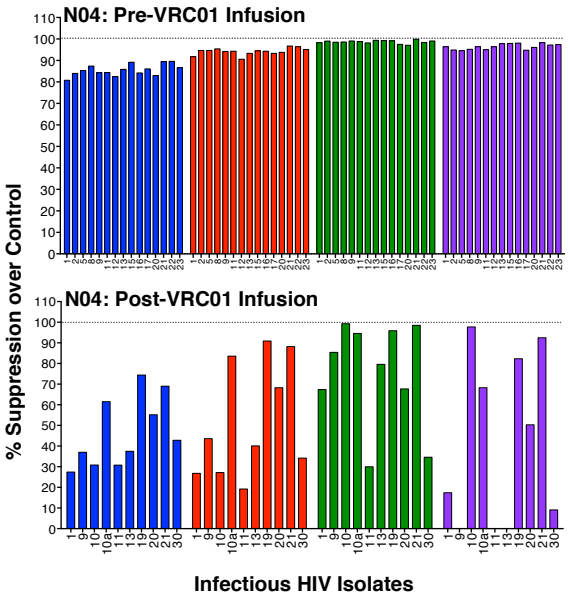


**N04 $IC_{80}$ (μg/mL)**

| Time Point | Infectious HIV Isolates | VRC01 | 3BNC117 | 10-1074 | PGT121 |
|---|---|---|---|---|---|
| Pre-VRC01 Infusion | 1 | 15.95 | 8.45 | 1.64 | 3.13 |
| | 2 | 21.34 | 8.58 | 1.47 | 8.3 |
| | 9 | 17.25 | 7.82 | 1.45 | 5.5 |
| Post-VRC01 Infusion | 1 | >40 | >40 | >40 | >40 |
| | 21 | 22.44 | 9.97 | 1.71 | 12.05 |
| | 30 | >40 | >40 | >40 | >40 |

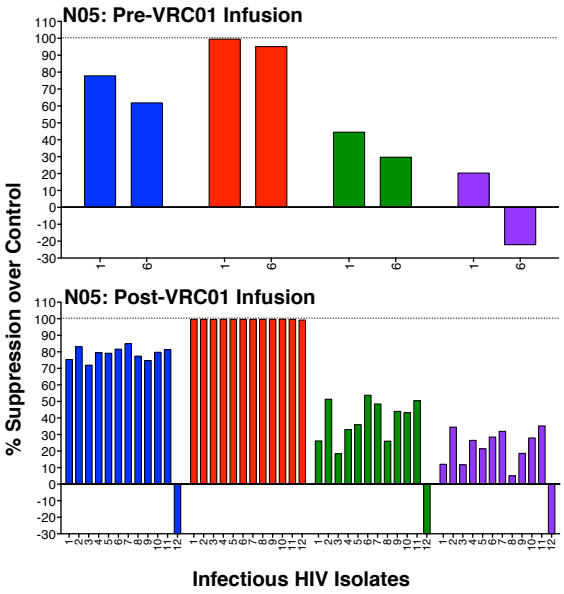


**N05 $IC_{80}$ (μg/mL)**

| Time Point | Infectious HIV Isolates | VRC01 | 3BNC117 | 10-1074 | PGT121 |
|---|---|---|---|---|---|
| Pre-VRC01 | 1 | 31.70 | 1.91 | >40 | >40 |
| Infusion | 6 | 23.58 | 1.58 | >40 | >40 |
| Post-VRC01 | 3 | 28.00 | 1.40 | >40 | >40 |
| Infusion | 6 | 14.92 | 1.30 | >40 | >40 |
| | 7 | 9.83 | 1.07 | >40 | >40 |
| | 12 | 38.13 | 2.31 | >40 | >40 |

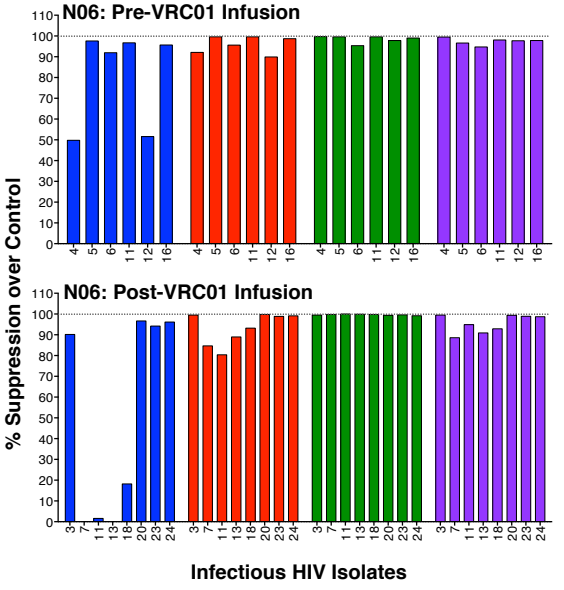


**N06 $IC_{80}$ (μg/mL)**

| Time Point | Infectious HIV Isolates | VRC01 | 3BNC117 | 10-1074 | PGT121 |
|---|---|---|---|---|---|
| Pre-VRC01 | 4 | 20.30 | 5.37 | 0.56 | 0.19 |
| Infusion | 5 | 7.45 | 1.92 | 0.38 | 0.53 |
| Infusion | 12 | 27 | 5.62 | 1.35 | 0.318 |
| Post-VRC01 | 7 | >40 | 8.87 | 0.56 | 8.50 |
| Infusion | 11 | >40 | 9.34 | 0.53 | 3.25 |
| | 13 | >40 | 9.80 | 0.60 | 9.46 |

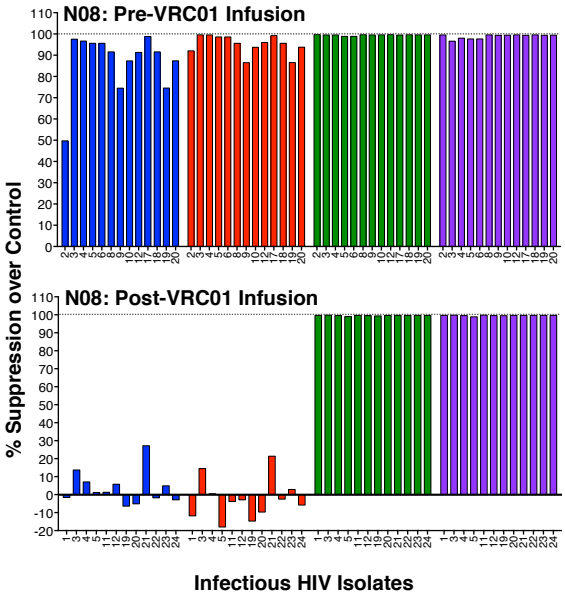


**N08 $IC_{80}$ (μg/mL)**

| Time Point | Infectious HIV Isolates | VRC01 | 3BNC117 | 10-1074 | PGT121 |
|---|---|---|---|---|---|
| Pre-VRC01 Infusion | 2 | 5.45 | 5.70 | 0.35 | 0.31 |
| | 3 | 4.93 | 4.43 | 0.20 | 0.17 |
| | 4 | 4.75 | 5.38 | 0.29 | 0.24 |
| | 9 | 4.68 | 3.70 | 0.29 | 0.22 |
| | 10 | 5.61 | 3.95 | 0.32 | 0.27 |
| Infusion | 19 | 5.42 | 4.60 | 0.37 | 0.27 |
| Post-VRC01 Infusion | 1 | >50 | >50 | 0.26 | 0.28 |
| | 3 | >50 | >50 | 0.19 | 0.11 |
| | 4 | >50 | >50 | 0.22 | 0.19 |
| | 5 | >50 | >50 | 0.27 | 0.18 |
| | 12 | >50 | >50 | 0.21 | 0.15 |
| | 21 | >50 | >50 | 0.24 | 0.14 |

VRC01
3BNC117
10-1074
PGT121

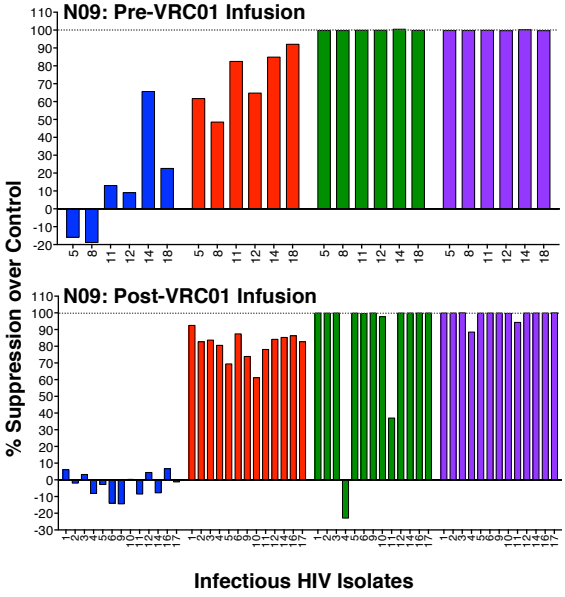


**N09 $IC_{80}$ (μg/mL)**

| Time Point | Infectious HIV Isolates | VRC01 | 3BNC117 | 10-1074 | PGT121 |
|---|---|---|---|---|---|
| Pre-VRC01 Infusion | 5 | >40 | 18.30 | 0.37 | 0.28 |
| | 8 | >40 | 22.99 | 0.43 | 0.33 |
| | 11 | >40 | 16.14 | 0.40 | 0.29 |
| | 12 | >40 | 23.03 | 0.49 | 0.39 |
| Post-VRC01 Infusion | 3 | >40 | 13.43 | 0.15 | 0.15 |
| | 4 | >40 | 16.22 | >40 | >40 |
| | 5 | >40 | 30.41 | 0.37 | 0.33 |
| | 12 | >40 | 20.78 | 0.40 | 0.35 |

VRC01
3BNC117
10-1074
PGT121

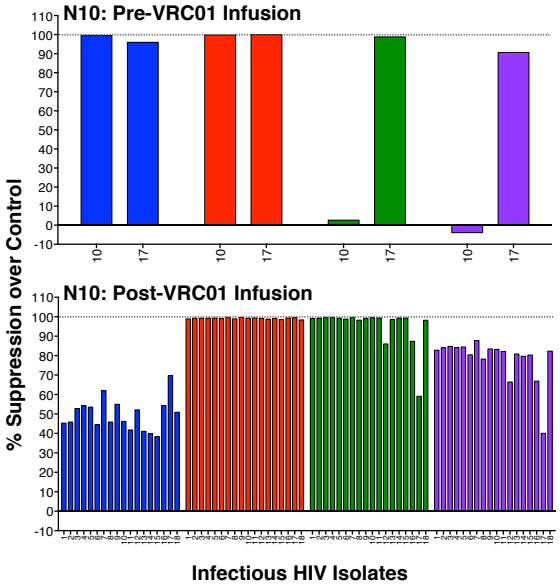


**N10 $IC_{80}$ (μg/mL)**

| Time Point | Infectious HIV Isolates | VRC01 | 3BNC117 | 10-1074 | PGT121 |
|---|---|---|---|---|---|
| **Pre-VRC01** | **10** | 2.35 | 0.48 | >40 | >40 |
| **Infusion** | **17** | 7.13 | 0.67 | 4.19 | 16.66 |
| **Post-VRC01** | **1** | >40 | 4.27 | 4.70 | 9.28 |
| **Infusion** | **2** | >40 | 4.10 | 3.70 | 15.14 |
| | **14** | >40 | 4.08 | 4.20 | 10.32 |
| | **15** | >40 | 4.59 | 3.58 | 10.26 |

Neutralization of pre- and post-infusion HIV isolates by VRC01 and other bNAbs (3BNC117, 10-1074, and PGT121) is shown in bar graphs. Numbers under the bars indicate individual infectious HIV isolates. $IC_{80}$ values in the accompanying table were independently determined for several isolates and bNAbs shown.

**Supplementary References**

1. Ledgerwood JE, Coates EE, Yamshchikov G, et al. Safety, pharmacokinetics and neutralization of the broadly neutralizing HIV-1 human monoclonal antibody VRC01 in healthy adults. Clinical and experimental immunology 2015;182:289-301.

2. Lynch RM, Boritz E, Coates EE, et al. Virologic effects of broadly neutralizing antibody VRC01 administration during chronic HIV-1 infection. Sci Transl Med 2015;7:319ra206.

3. Li JZ, Etemad B, Ahmed H, et al. The size of the expressed HIV reservoir predicts timing of viral rebound after treatment interruption. Aids 2016;30:343-53.

4. Keele BF, Giorgi EE, Salazar-Gonzalez JF, et al. Identification and characterization of transmitted and early founder virus envelopes in primary HIV-1 infection. Proc Natl Acad Sci U S A 2008;105:7552-7.

5. Li H, Bar KJ, Wang S, et al. High Multiplicity Infection by HIV-1 in Men Who Have Sex with Men. PLoS pathogens 2010;6:e1000890.

6. Larkin MA, Blackshields G, Brown NP, et al. Clustal W and Clustal X version 2.0. Bioinformatics 2007;23:2947-8.

7. Guindon S, Dufayard JF, Lefort V, Anisimova M, Hordijk W, Gascuel O. New algorithms and methods to estimate maximum-likelihood phylogenies: assessing the performance of PhyML 3.0. Syst Biol 2010;59:307-21.

8. Darriba D, Taboada GL, Doallo R, Posada D. jModelTest 2: more models, new heuristics and parallel computing. Nature methods 2012;9:772.

9. Cavanaugh JE. Unifying the derivations for the Akaike and corrected Akaike information criteria. Statist Probab Lett 1997;33:201-8.

10. Deng W, Maust BS, D.C. N, et al. DIVEIN: a web server to analyze phylogenies, sequence divergences, diversity and informative sites. Bio Techniques 2010;48:405-8.

11. Slatkin M, Maddison WP. A cladistic measure of gene flow inferred from the phylogenies of alleles. Genetics 1989;123:603-13.

12. Pond SL, Frost SD, Muse SV. HyPhy: hypothesis testing using phylogenies. Bioinformatics 2005;21:676-9.

13. Hudson RR. A new statistic for detecting genetic differentiation. Genetics 2000;155:2011-4.

14. Lee HY, Giorgi EE, Keele BF, et al. Modeling sequence evolution in acute HIV-1 infection. Journal of theoretical biology 2009;261:341-60.

15. Giorgi EE, Bhattacharya T. A note on two-sample tests for comparing intra-individual genetic sequence diversity between populations. Biometrics 2012;68:1323-6; author reply 6.

16. Hraber P, Korber B, Wagh K, et al. Longitudinal Antigenic Sequences and Sites from Intra-Host Evolution (LASSIE) Identifies Immune-Selected HIV Variants. Viruses 2015;7:5443-75.

17. Zhou T, Georgiev I, Wu X, et al. Structural basis for broad and potent neutralization of HIV-1 by antibody VRC01. Science 2010;329:811-7.

18. Lee FH, Mason R, Welles H, et al. Breakthrough Virus Neutralization Resistance as a Correlate of Protection in a Nonhuman Primate Heterologous Simian Immunodeficiency Virus Vaccine Challenge Study. Journal of virology 2015;89:12388-400.

19. Wang CY, Sawyer LS, Murthy KK, et al. Postexposure immunoprophylaxis of primary isolates by an antibody to HIV receptor complex. Proc Natl Acad Sci U S A 1999;96:10367-72.

20. Salazar-Gonzalez JF, Bailes E, Pham KT, et al. Deciphering human immunodeficiency virus type 1 transmission and early envelope diversification by single-genome amplification and sequencing. J Virol 2008;82:3952-70.

21. Tamura K, Stecher G Fau - Peterson D, Peterson D Fau - Filipski A, Filipski A Fau - Kumar S, Kumar S. MEGA6: Molecular Evolutionary Genetics Analysis version 6.0. Mol Biol Evol 2013;30:2725-9 LID - 10.1093/molbev/mst197 [doi].

22. Chuang GY, Liou D, Kwong PD, Georgiev IS. NEP: web server for epitope prediction based on antibody neutralization of viral. Nucleic Acids Res 2014;42:W64-71 LID - 10.1093/nar/gku318 [doi].

23. Chuang GY, Acharya P Fau - Schmidt SD, Schmidt Sd Fau - Yang Y, et al. Residue-level prediction of HIV-1 antibody epitopes based on neutralization of. J Virol 2013;87:10047-58 LID - 10.1128/JVI.00984-13 [doi].

24. Maydt J, Lengauer T. Recco: recombination analysis using cost optimization. Bioinformatics 2006;22:1064-71.

25. Wu X, Yang ZY, Li Y, et al. Rational design of envelope identifies broadly neutralizing human monoclonal antibodies to HIV-1. Science 2010;329:856-61.